Symposium B, Apri. 2004, San Francisco, CA
Mat. Res. Soc. Symp. Proc. Vol. 809 © 2004 Materials Research Society

Interference-enhanced Raman Scattering in Strain Characterization of Ultra-thin Strained SiGe and Si Films on Insulator

Haizhou Yin[1], K.D. Hobart[2], S.R. Shieh[3], R.L. Peterson[1], T.S. Duffy[3], and J.C. Sturm[1]
[1]Princeton Institute for the Science and Technology of Materials (PRISM) and
Department of Electrical Engineering, Princeton University, Princeton, NJ 08544
[2]Naval Research Laboratory, Washington, DC 20357
[3]Department of Geosciences, Princeton University, Princeton, NJ 08544

ABSTRACT

Interference-enhanced Raman scattering was utilized to characterize strain in ultra-thin strained silicon-germanium (SiGe) and silicon layers on insulator. Strained SiGe and silicon films with thickness ranging from 10 to 30 nm on insulating borophosphorosilicate glass (BPSG) were formed by layer transfer techniques and/or strain manipulation via lateral expansion of strained films. The optical interference of the multiple reflections at the BPSG interfaces can substantially boost the reflectivity at the interfaces. The reflection improves Raman signal from SiGe and/or silicon films by increasing excitation intensity and Raman signal collection in the thin films. With the use of interference-enhanced Raman scattering, strain can be characterized at visible wavelengths for films as thin as 10 nm.

INTRODUCTION

Strain-induced carrier transport enhancement draws a growing interest for electronic applications as device scaling, the conventional scheme used for CMOS device improvement for the last several decades, faces formidable difficulties as it enters the sub-100 nm gate length regime. Electron mobility is considerably enhanced in strained Si whereas strained SiGe is more effective for hole mobility enhancement [1,2]. Silicon-on-insulator (SOI) structures have many desirable properties, such as reduced parasitic capacitance, lower leakage current and easy fabrication of multi-gate structures. Therefore, it is attractive to combine SOI with stained Si and/or SiGe layers. Recently, fabrication and device characterization on SiGe on insulator (SGOI) and strained-Si directly on insulator (SSDOI) have been reported [3-7]. The total thickness of semiconducting layers on insulator needs to be thin in order to suppress short channel effects in small devices [7].

Raman scattering is a non-destructive and widely used means in strain characterization [8]. The major challenge in utilizing Raman scattering to characterize strain in thin films is the Raman sensitivity at different excitation wavelengths. For example, when long wavelength excitation is employed, a thick film is required to generate enough Raman signal because of the large optical penetration depth [9]. To measure strain in thin films, ultra-violet (UV) excitation has been used for its shallow penetration [10]. But UV excitation has its own limits. It is not capable of probing strain in multiple thin films as the top thin film can completely absorb the excitation beam due to the its small penetration depth. In addition, the excitation beam can not reach the substrate, so the substrate Raman peak, which could have served as a perfect reference point, is missing.

In this paper, long wavelength excitation is employed to induce Raman scattering in single or multiple ultra-thin films on top of an insulating layer made of viscous

borophosphorosilicate glass (BPSG). The interference-enhanced reflection at BPSG interfaces for long wavelength excitation overcomes the limits of the UV-Raman mentioned above by boosting the Raman signal from thin films on insulator.

EXPERIMENTS AND DISCUSSIONS

Thin silicon and SiGe films with various strain on BPSG have recently been demonstrated using wafer bonding and Smart-cut® processes [11-13]. High-quality, fully-relaxed Si0.7Ge0.3 films have been obtained through a process which does not fundamentally require misfit dislocations. The fabrication process is the same as Ref. 11 and is briefly described as follows: a 30-nm $Si_{0.7}Ge_{0.3}$ film, which was commensurately strained to bulk Si(100), was transferred onto a 200-nm BPSG film (4.4% B and 4.1% P by weight) on a silicon wafer, and then patterned into islands with edge length ranging from 20 to 200 μm. No strain relaxation took place during the layer transfer, since the highest process temperature was 550°C, at which the BPSG film remained rigid. When SiGe islands were then annealed at 800°C, the BPSG film softened (a viscosity of 1.2 x 10^{11} Poise at 800°C) and the as-bonded, compressively-strained $Si_{0.7}Ge_{0.3}$ film started to relax by macroscopic lateral expansion. In some cases, a Si/SiGe bi-layer was transferred onto BPSG for generating tensile strain in the Si film: when BPSG turned soft at a high-temperature anneal, the compressive stress in the SiGe film drove the island lateral expansion and put the Si film under tension. The lateral expansion stopped when the compressive stress in the SiGe film was balanced by the tensile stress in the Si film [13]:

$$\frac{E_{SiGe}}{1-\nu_{SiGe}}\varepsilon_{SiGe}h_{SiGe}+\frac{E_{Si}}{1-\nu_{Si}}\varepsilon_{Si}h_{Si}=0, \quad (1)$$

where E, ν, ε, and h represent the Young's Modulus, Possion's ratio, strain, and the film thickness, respectively.

The micro-Raman station used in this work has a backscattered configuration. The normal incident excitation beams (wavelengths of 514.5 nm and 488 nm) are focused by a microscope objective lens onto a spot of 3 micron in diameter. The backscattered Raman signal is then collected by the same lens. The strain $\varepsilon_{Ge=30\%}$ in the $Si_{0.7}Ge_{0.3}$ film and the strain ε_{Si} in the Si film were inferred from the optical phonon frequencies $\omega_{Si\text{-}Si}$ by [8,14]

$$\omega_{Si\text{-}Si}(Si_{0.7}Ge_{0.3}) = 499\ cm^{-1} - 815\varepsilon_{Ge=30\%}\ cm^{-1}, \quad (2)$$

$$\omega_{Si\text{-}Si}(Si) = 520\ cm^{-1} - 715\varepsilon_{Si}\ cm^{-1}. \quad (3)$$

Figure 1 shows the Raman spectra taken on 30-nm strained $Si_{0.7}Ge_{0.3}$ with different BPSG thicknesses using a visible 514-nm excitation laser. For the sample without BPSG, the SiGe Raman peak (512 cm^{-1}) was much weaker than the silicon substrate Raman peak (520 cm^{-1}), which suggests that most of the Raman signal comes from the silicon substrate. This is consistent with the large penetration depth (~ 340 nm) for the 514-nm wavelength. The small SiGe Raman peak, obscured by the strong substrate Raman peak, makes it difficult to accurately determine the peak position and thus strain value. When a 225-nm BPSG layer was sandwiched between the SiGe film and the substrate, the substrate Raman peak was greatly reduced whereas the SiGe Raman peak was enhanced (Fig. 1). The height ratio of the SiGe Raman peak to the

https://doi.org/10.1557/PROC-809-B3.6

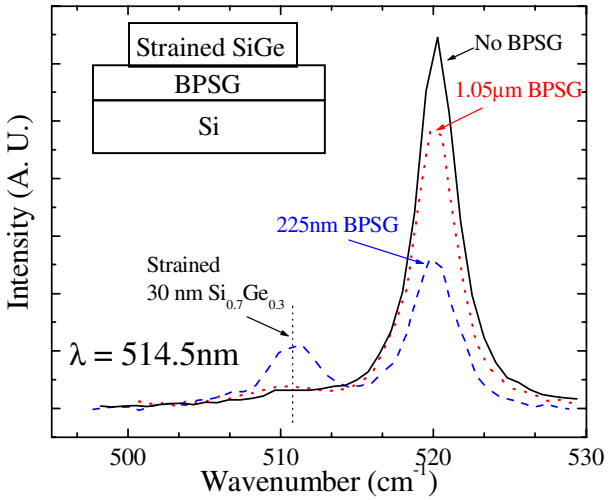

Figure 1. Measured Raman spectra of fully-strained 30-nm $Si_{0.7}Ge_{0.3}$ with various BPSG thickness

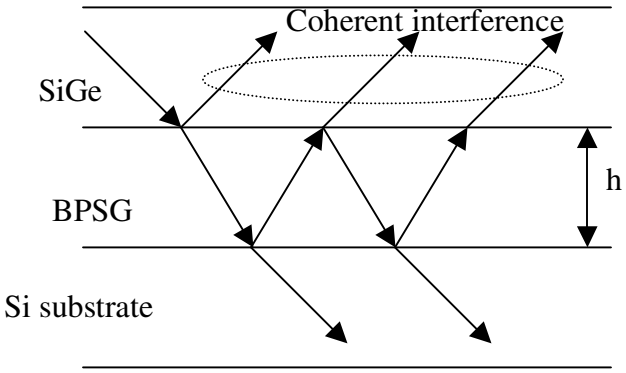

Figure 2. Schematic diagram of the multiple reflections at the BPSG interfaces. The reflected light gives rise to optical interference.

substrate Raman peak increased by about ten times compared to the BPSG-free sample and the SiGe Raman peak position could be readily determined. However, when the BPSG thickness was 1.05 μm, no enhancement of the height ratio was observed and the BPSG layer had a negligible effect on the Raman measurement.

To understand the effect of BPSG on Raman measurement, the light reflection at BPSG interfaces needs to be identified. The sandwiched BPSG film forms two reflection interfaces: SiGe/BPSG and BPSG/Si-substrate. The reflectivity at a single SiGe/BPSG interface for normal incident light is $R_{SiGe/BPSG} = (n_{BPSG} - n_{SiGe})^2 / (n_{BPSG} + n_{SiGe})^2$, where n represents refractive index [15]. In contrast, the reflectivity of SiGe/BPSG/Si-substrate (SiGe/BPSG and BPSG/Si-substrate interfaces) is much more complex owing to the optical interference of the multiple reflections (Fig. 2). The interference can be either constructive or destructive and depends on the phase shift $\delta = 2\pi n_{BPSG} h / \lambda$, where h and λ are the BPSG thickness and excitation wavelength, respectively. Given the similarity between the SiGe/BPSG/Si-substrate and the well-known Fabry-Perot structure [15], the reflectivity formula of the Fabry-Perot structure can be applied to SiGe/BPSG/Si-substrate:

$$R_{SiGe/BPSG/Si} = F \sin^2 \delta / (1 + F \sin^2 \delta), \quad (4)$$

where F is defined as $4R_{Si/BPSG} / (1 - R_{Si/BPSG})^2$. For simplicity, the refractive index is assumed the same for silicon and SiGe. The silicon refractive index is 4.22 and 4.35 for excitation wavelengths 514.5 nm and 488 nm, respectively. The BPSG refractive index is 1.46 at both excitation wavelengths. Figure 3 depicts the calculated BPSG thickness dependence of the reflectivity for 514.5-nm excitation. When the multiple reflections are in phase and thus constructively interfere, the reflectivity of the SiGe/BPSG/Si structure reaches the maximum value of 0.62, which is nearly three times the reflectivity (0.24) at a single SiGe/BPSG interface.

The reflection at the BPSG interfaces affects the Raman measurement by increasing the observed Raman signal from the SiGe film while suppressing the observed Raman signal from the substrate. The underlying mechanism lies on two factors. First, as a result of the reflection,

https://doi.org/10.1557/PROC-809-B3.6

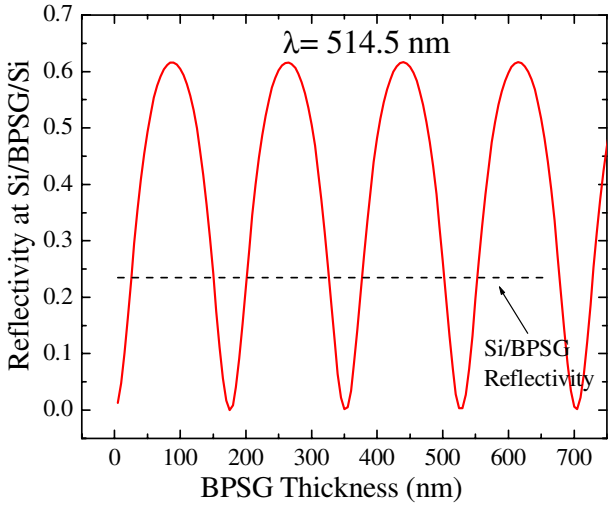

Figure 3. Calculated Si/BPSG/Si-substrate reflectivity as a function of BPSG thickness

the excitation intensity in the SiGe film is increased and the excitation intensity in the substrate is reduced (Figure 2). Since Raman scattering is linearly proportional to the excitation intensity, the Raman signal intensity from the SiGe film increases and that from the substrate decreases. After taking into account of the multiple reflections at the SiGe/air and SiGe/BPSG/Si interfaces, the enhancement in the excitation intensity ratio of the SiGe film to the substrate can be expressed in terms of reflectivity at the interfaces as

$$(1+R_{SiGe/BPSG/Si}R_{SiGe/Air})/\{(1-R_{SiGe/BPSG/Si}R_{SiGe/Air})(1-R_{SiGe/BPSG/Si})\}, \quad (5)$$

which varies from unity for $R_{SiGe/BPSG/Si}$=0 to 5.5 for $R_{SiGe/BPSG/Si}$=0.62. The light absorption in the SiGe film is not included in Eq. (5), which is a reasonable approximation since the SiGe thickness (30 nm) is far less than the optical penetration depth (~340 nm). The second contribution enhancing the Raman intensity ratio of the SiGe film to the substrate by the reflection at SiGe/BPSG/Si relies on the improved Raman signal collection from the SiGe film while reducing Raman signal collection from the substrate. Some Raman scattered light in the SiGe film that would otherwise have been absorbed in the substrate is reflected by the SiGe/BPSG/Si interfaces and then detected. On the other hand, since only part of the Raman signal in the substrate is transmitted past the interfaces to be detected, the observable Raman scattered light from the substrate is reduced. The enhancement in the Raman signal collection ratio of the SiGe film to the substrate is

$$(1+R_{SiGe/BPSG/Si})/(1-R_{SiGe/BPSG/Si}) \ . \quad (6)$$

Combining the excitation intensity enhancement and Raman signal collection enhancement, one can estimate the total enhancement in Raman peak ratio of the SiGe film to the substrate by multiplying Eq. (5) and Eq. (6). Figure 4 shows the calculated Raman peak ratio enhancement as a function of the BPSG thickness for two excitation wavelengths. The SiGe Raman peak height can be enhanced by more than twenty times relative to the substrate Raman peak.

The strong change in Raman signal intensity with BPSG thickness shown in Fig. 2 can be predicted using Eqs. (5) and (6). At 514.5-nm excitation, the Raman signal ratio enhancement for SiGe/BPSG/Si-substrate samples over the SiGe/Si-substrate sample is calculated to be 10.3 and 1 for 225-nm and 1.05-μm BPSG, respectively. The observed ratio enhancement in Fig 2 is 10.6 and 1.3 for the two BPSG thicknesses, in good agreement with the calculation. The small ratio enhancement measured for 1.05-μm BPSG is owing to the out-of-phase reflections at 514.5-nm excitation. When the excitation wavelength is changed from 514.5 nm to 488 nm, the multiple reflections are no longer out of phase and the ratio enhancement is calculated to be 13.2, in line with the observed value of 12 (Fig. 5). This suggests that the excitation wavelength is a

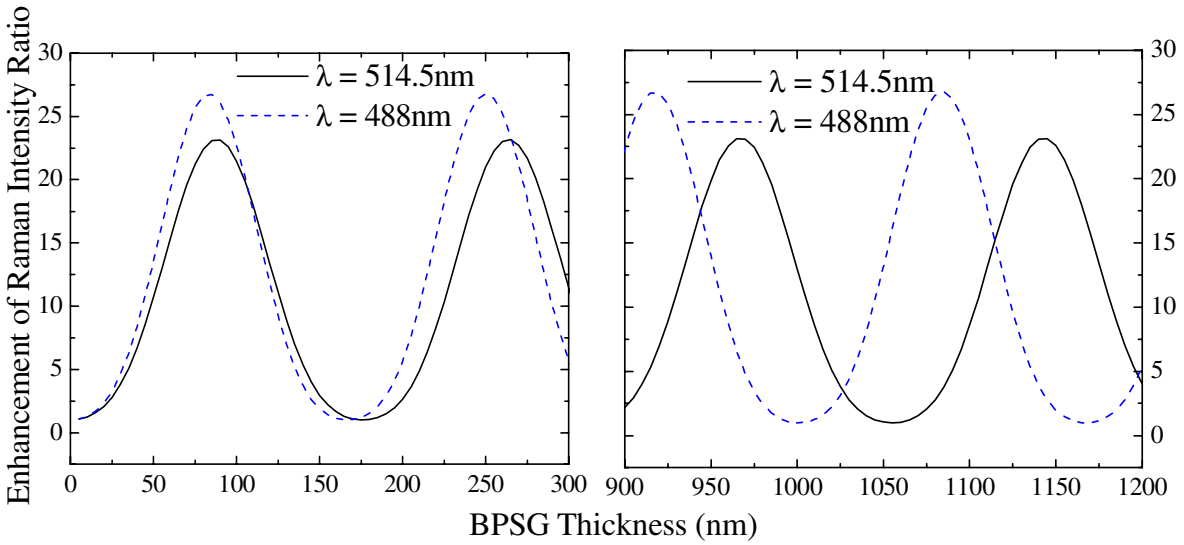

Figure 4. Calculated enhancement in Raman intensity ratio of the SiG film to the silicon substrate as a function of BPSG thickness for two excitation wavelengths.

convenient adjustable parameter for maximizing the interference enhancement in Raman scattering.

Since the interference-enhanced Raman scattering applies to all films above the reflection interfaces, as can be seen in Fig. 2, this method is uniquely suitable for measuring multiple thin films on insulator, which is beyond reach of UV-Raman due to its shallow optical penetration depth. As an illustration of this unique capability, a bi-layer structure of compressive 30-nm $Si_{0.7}Ge_{0.3}$ and tensile 10-nm Si on insulator was measured at 514.5-nm and 488-nm excitation

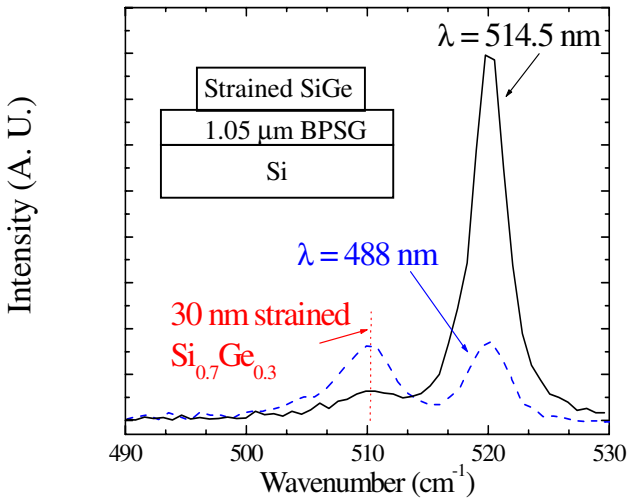

Figure 5. Measured Raman spectra of 30-nm $Si_{0.7}Ge_{0.3}$/1.05 μm BPSG for two excitation wavelengths

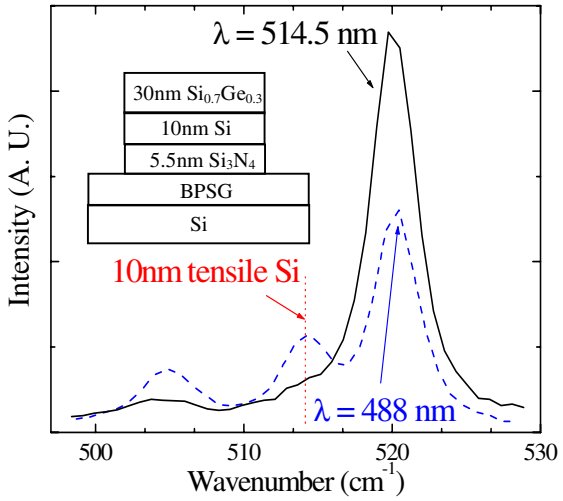

Figure 6. Measured Raman spectra of 30-nm $Si_{0.7}Ge_{0.3}$/10-nm Si/5.5-nm Si_3N_4 on 1.05 μm BPSG.

(Fig. 6). Even though the strained-Si film is very thin and is covered by a 30-nm SiGe film, the Raman peak from the strained-Si film is strong, indicating 0.7% tensile strain.

CONCLUSIONS

Interference-enhanced Raman scattering was studied for strain characterization of ultra-thin strained Si/SiGe layers on insulating BPSG. The significant increase in Raman signal from the thin films compared to the substrate was attributed to reflections at the SiGe/BPSG and BPSG/Si-substrate interfaces. The reflectivity of the structure is determined by the optical interference of the multiple reflections and has a strong dependence on BPSG thickness and excitation wavelength. By adjusting the excitation wavelength to achieve constructive interference, strain in multiple thin films can be measured by Raman scattering at visible wavelengths.

ACKNOWLEDGEMENT

The authors would like to thank Steven Lyon at Princeton University for helpful discussions and Tony Margarella at Northrop-Grumman for deposition of BPSG films. This work is supported by DARPA(N66001-00-10-8957) and ARO(DAAG55-98-1-0270).

REFERENCES

1. K. Ismail, M. Arafa, K. L. Saenger, J. O. Chu, and B. S. Meyerson l, *Appl. Phys. Lett.* **66**, 1077 (1995)
2. Y. H. Xie, Don Monroe, E. A. Fitzgerald, P. J. Silverman, F. A. Thiel, and G. P. Watson, *Appl. Phys. Lett.* **63**, 2263 (1993)
3. T. Tezuka, N. Sugiyama, and S. Takagi, *Appl. Phys. Lett.* **79** (12), 1798-1800 (2001).
4. Z. Y. Cheng, M. T. Currie, C. W. Leitz *et al.*, *IEEE Electron Device Lett.* **22** (7), 321-323 (2001).
5. L. J. Huang, J. O. Chu, S. A. Goma *et al.*, *IEEE Trans. Electron Devices* **49**, 1566 (2002).
6. H. Yin, K. D. Hobart, R. L. Peterson, F. J. Kub, S. R. Shieh, T. S. Duffy and J. C. Sturm, Int. Electron Devices Meeting (IEDM 2003) Tech. Dig., pp. 3.2.1 - 3.2.4. (2003)
7. K. Rim, K. Chan, L. Shi *et al.*, Int. Electron Devices Meeting (IEDM 2003) Tech. Dig., pp. 3.1.1 - 3.1.4. (2003)
8. J.C. Tsang, P.M. Mooney, F. Dacol, and J.O. Chu, J. Appl. Phys. **75**, 8098 (1994)
9. D.E. Aspnes *et. al., Phys. Rev.* B **27**, 985 (1983)
10. T. S. Drake, C. Ní Chléirigh, M. L. Lee, A. J. Pitera, E. A. Fitzgerald, *et al.*, *Appl. Phys. Lett.* 83, 875 (2003)
11. K.D. Hobart, F.J. Kub, M. Fatemi, M.E. Twigg, P.E. Thompson, T.S. Kuan, and C.K. Inoki, *J. Electron. Mater.* **29**, 897 (2000).
12. H. Yin, R. Huang, K.D. Hobart, Z. Suo, T.S. Kuan, C.K. Inoki, S.R. Shieh, T.S. Duffy, F.J. Kub, and J.C. Sturm, *J. Appl. Phys.* **91**, 9716 (2002).
13. H. Yin, K.D. Hobart, F.J. Kub, S.R. Shieh, T.S. Duffy, and J.C. Sturm, *Appl. Phys. Lett.* **82**, 3853 (2003).
14. D.J. Lockwood and J.-M. Baribeau, *Phys. Rev.* B **45**, 8565 (1992)
15. M. Born and E. Wolf, *Principles of optics.* Pergmon, New York (1980)